Journal of Zhejiang University-SCIENCE B (Biomedicine & Biotechnology)
ISSN 1673-1581 (Print); ISSN 1862-1783 (Online)
www.zju.edu.cn/jzus; www.springerlink.com
E-mail: jzus@zju.edu.cn

Growth factors induce the improved cardiac remodeling in autologous mesenchymal stem cell-implanted failing rat hearts*

Ze-wei TAO†, Long-gui LI†‡, Zhao-hua GENG, Tao DANG, Shan-jun ZHU

(*Department of Cardiovascular Diseases, Xinqiao Hospital, Third Military Medical University, Chongqing 400037, China*)

†E-mail: taozw@hotmail.com; lgli602@163.com

Received Aug. 9, 2009; Revision accepted Jan. 27, 2010; Crosschecked Mar. 10, 2010

Abstract: Therapeutically delivered mesenchymal stem cells (MSCs) improve ventricular remodeling. However, the mechanism underlying MSC cardiac remodeling has not been clearly determined. Congestive heart failure (CHF) was induced in rats by cauterization of the left ventricular free wall. MSCs were cultured from autologous bone marrow and injected into the border zone and the remote myocardium 5 d after injury. Ten weeks later, when compared with sham operation, CHF significantly increased nucleus mitotic index, capillary density, and expression of insulin-like growth factor 1, hepatocyte growth factor and vascular endothelial growth factor in the border zone (P<0.01) and decreased each of them in the remote myocardium (P<0.05 or P<0.01). MSC implantation in CHF dramatically elevated expression of these growth factors in the remote myocardium and further elevated their expression in the border zone when compared with CHF without MSC addition (P<0.05 or P<0.01). This was paralleled by a higher nucleus mitotic index and a significantly increased capillary density both in the remote myocardium and in the border zone, and by a lower percentage of area of collagen and a higher percentage of area of myocardium in the border zone (P<0.05 or P<0.01), and cardiac remodeling markedly improved. Autologous MSC implantation promoted expression of growth factors in rat failing myocardium, which might enhance cardiomyogenesis and angiogenesis, and improved cardiac remodeling.

Key words: Mesenchymal stem cells, Growth factor, Myocardium, Cardiac remodeling
doi:10.1631/jzus.B0900244 **Document code:** A **CLC number:** R54

1 Introduction

Congestive heart failure (CHF) is a major worldwide epidemic. Its incidence and prevalence have continued to increase with aging of the population and improvement of acute myocardial infarction (Hunt, 2005). Failing myocardium is characterized by cardiac hypertrophy, insufficient vascularization, and cardiomyocyte loss. Although treatment of CHF has improved, approaches (Tao and Li, 2007) that aim to promote myogenesis and angiogenesis are attractive and promising new therapies.

Mesenchymal stem cells (MSCs) are adult tissue multipotential stem cells and are the main type of hematopoiesis-supportive stromal cells in bone marrow. They are readily accessible from bone marrow, adipose tissue and skeletal muscle, and there are no ethical and immunological complications when applied in cell therapy. Animal studies (Amado *et al*., 2005), preclinical trials (Amado *et al*., 2006), and early clinical experience (Chen *et al*., 2004) support the concept that therapeutically delivered MSCs can safely improve ventricular remodeling and heart function.

The mechanism of action underlying MSCs-based therapy has not been clearly determined. To investigate the effects of MSC implantation on cardiac remodeling, we injected autologous MSCs intramyocardially into the border zone and the remote

‡ Corresponding author
* Project (No. 20060400200) supported by the China Postdoctoral Science Foundation

myocardium in CHF rats, detected cells with 4′, 6-diamino-2-phenylindole (DAPI) positive staining nuclei, analyzed bioactive and mitogenic factors and nucleus mitotic index, and evaluated vascular density and area percentages of collagen and myocardium.

2 Materials and methods

All animal manipulations were performed in accordance with institutional guidelines of the Third Military Medical University Animals Research Committee and conformed with the Guide for the Care and Use of Laboratory Animals published by the US National Institutes of Health (NIH Publication No. 85-23, revised 1985).

2.1 Isolation and expansion of MSCs

Sixty male Sprague-Dawley rats weighing (350±30) g were anesthetized with a combination of ketamine (75 mg/kg) and xylazine (10 mg/kg) (i.p.), after which bone marrow was aspirated from the shafts of both femurs with an 18-gauge needle attached to a 10-ml syringe containing 1 ml of heparinized phosphate buffered saline (PBS). Bone marrow cells were centrifuged, the heparinized PBS removed, and the pellets transferred into a 12.5-cm^2 flask containing Dulbecco's modified Eagle's medium (DMED)/F12 (Hyclone) supplemented with 10% (v/v) fetal bovine serum (Gibco) and cultured at 37 °C in humid air with 5% CO_2. The medium was replaced to remove the nonadherent bone marrow cells after the first 24 h in culture and every 3 d thereafter. Each primary culture was replated to a 25-cm^2 flask when MSCs reached about 80% confluency by digesting the cells with pre-warmed 0.125% (w/v) trypsin (Sigma) for 2 to 5 min at room temperature. The detached MSCs were centrifuged and the pellets were introduced into a 75-cm^2 fresh flask for the second culture passage. Homogeneous MSCs (approximately 5×10^6) were obtained with these two passages and used for cell transplantation. Six animals were excluded from the study because of femoral fractures.

2.2 Fluorescence-activating cell sorting (FACS) analysis of MSCs

Prior to the experiments, the MSC population after two passages was determined by fluorescence-activating cell sorting (FACS; Beckman Coulter, Fullerton, CA, USA) analysis using directly conjugated mouse anti-rat monoclonal antibodies against CD44H (fluorescein isothiocyanate (FITC) conjugated, BD Biosciences), CD45 (phycoerythrin (PE)-Cy5-conjugated, BD Biosciences), and CD90 (FITC-conjugated, BD Biosciences). A matching FITC-conjugated mouse immunoglobulin G2a (IgG2a) antibody (BD Biosciences) and a matching PE-Cy5-conjugated mouse IgG1 antibody (BD Biosciences) were used as isotype controls.

2.3 CHF model

Myocardial injury was produced by cauterization 5 d before MSC implantation. As previously described (Tao *et al*., 2005), rats were anesthetized with pentobarbital (40 mg/kg, i.p.), intubated, and ventilated with room air on a rodent ventilator. The heart was exposed via a 2-cm incision at the third intercostal space, and the myocardium within the left ventricular (LV) free wall was cauterized with an electronic cautery unit (the surface area is about 50 mm^2). Cauterization injury was made 2 times for 4 s when the cautery unit is as hot as it can melt tin. After cauterization, the incision was closed and rats were allowed to recover (six animals died from the procedure). Sham-operated animals (n=15) were treated with the same surgical procedure but without injury to the heart (all animals recovered).

2.4 MSC labeling and implantation

Before implantation, MSCs were cultured in DAPI (Roche) culture medium (50 μg/ml) for 30 min to facilitate subsequent identification as previously described (Davani *et al*., 2003). After quickly washing the cells in five changes of PBS to remove unincorporated DAPI, MSCs were collected and resuspended in 150 μl of PBS and stored on ice (<1 h) until implantation into the myocardium. Twenty-two CHF animals with their own specific successfully-cultured MSCs were anesthetized by pentobarbital (40 mg/kg, i.p.), intubated, and ventilated with room air on a rodent ventilator. The heart was exposed and the MSC suspension was injected with a 27-gauge needle into the border zone (3 injections, 30 μl each) and the remote myocardium (3 mm away and far from the scar border; 2 injections, 30 μl each) of the LV. The

remaining 26 CHF rats without their own specific successfully-cultured MSCs and sham-operated animals were injected with the same volume of PBS. These procedures caused 2, 3, and 0 deaths in CHF rats with MSCs, CHF rats with PBS, and sham-operated rats with PBS, respectively. After the implantation of MSCs, all the animals were inspected every day for the deceased ones in order to calculate survival rate.

2.5 Echocardiography

Ten weeks after MSC implantation, rats were anesthetized with pentobarbital (40 mg/kg, i.p.), and imaging was performed with a Philips iE33 echocardiography system fitted with an S12-4 transducer (USA). LV parameters were obtained from two-dimensional images and M-mode interrogation in a long-axis view as previously described (Tao *et al*., 2004), and then LV end-diastolic dimensions (LVEDd), ejection fraction (LVEF) and fractional shortening (LVFS), ejection time (ET), isovolumic contraction time (ICT), isovolumic relaxation time (IRT), and Tei index [(ICT+IRT)/ET] were calculated. All echocardiographic measurements were averaged from at least five separate cardiac cycles.

2.6 Hemodynamics

After the echocardiography measurements, a 2F high-fidelity, catheter-tipped micromanometer (model SPR-869, Millar Inc.) was inserted into the right carotid artery to record mean arterial pressure (MAP), and then advanced into the LV to record LV end-diastolic pressure (LVEDP), and the maximal rates of pressure development (dP/dt_{max}) and decline (dP/dt_{min}) using a PowerLab data acquisition system (AD instruments).

2.7 Cardiac morphology

After the hemodynamic measurements, the heart was arrested in diastole with 1 ml of 10% (w/v) KCl injected into the left atrium. Six hearts in the CHF rats with or without MSC treatment were digitally photographed for scars in the LV free wall. The great vessels, atria, and right ventricle were trimmed away, the anterior ventricular septum was cut, the LV extended, and scars on the epicardial and endocardial aspects photographed. The scar area on each side of the LV was manually traced by using Adobe Photoshop CS3 software to calculate the scar size on each heart. Scar size (mm^2)=(epicardial scar area+endocardial scar area)/2. A mid longitudinal cross-section slice about 2 mm thick was cut from six hearts in each group and fixed in 10% (w/v) formalin solution. The slice was then dehydrated and embedded in paraffin. One 4-μm thick section was obtained from this slice, mounted onto glass slide, and stained with Masson's trichrome. Six high power fields (×200) in the border zones of the sections in each group were visualized by Leica DMIRB fluorescence microscopy for measurement of area percentages of collagen and myocardium. Tissue from a transverse cross-section across the scar about 2 mm thick in LV was obtained and frozen in liquid N_2 and then stored at −80 °C in preparation for cryosectioning and immunohistochemical analysis. Each 50-mg block of myocardium from the border zone or the remote myocardium in LV was frozen in liquid N_2 and stored at −80 °C for total RNA isolation and total protein extraction.

2.8 SYBR green real-time reverse transcription-polymerase chain reaction (RT-PCR)

Total RNA was isolated from 50 mg of myocardium with TRIzol® reagent (Invitrogen). The primers for amplifying insulin-like growth factor 1 (IGF-1), hepatocyte growth factor (HGF), and vascular endothelial growth factor A (VEGF-A) are listed in Table 1. Glyceroldehydes-3-phosphate-dehydrogenase (GAPDH) was used as the internal-control gene. The SYBR green real-time RT-PCR amplifications were performed using SYBR® PrimeScript™ RT-PCR Kit (TaKaRa Biotech Co.) and Applied Biosystems 7500 System (Applied Biosystems, USA). The threshold cycle (C_t) value of each sample was averaged and then used for the $2^{-\Delta C_t}$ calculation. Using the $2^{-\Delta C_t}$ method, the data were presented as the fold change in gene expression normalized to the endogenous reference gene GAPDH.

2.9 Western blotting analysis

Total protein was extracted and stored at −20 °C until used for Western blotting analysis. For HGF expression analysis, the proteins were separated by 10% (w/v) glycine-sodium dodecyl sulfate polyacrylamide gel electropheresis (SDS-PAGE) and transferred to a 0.45-μm polyvinylidene fluoride

Table 1 Primers used for real-time RT-PCR assay

Gene	Primer sequences (5′-3′)	GenBank accession No.	T_m (°C)	Amplicon size (bp)
IGF-1	TCGGCCTCATAATACCCACTCTG-se CCGAGCTGGTAAAGGTGAGCA-as	NM178866	60	144
HGF	CGGAGCATCGCTACAGAATGAA-se CCACGACTTAGCGCCCACTTA-as	NM017017	60	138
VEGF-A	TCACCAAAGCCAGCACATAG-se GCTCACAGTGATTTTCTGGC-as	NM031836	60	101
GAPDH	GGCACAGTCAAGGCTGAGAATG-se ATGGTGGTGAAGACGCCAGTA-as	NM017008	60	143

IGF-1: insulin-like growth factor 1; HGF: hepatocyte growth factor; VEGF-A: vascular endothelial growth factor A; GAPDH: glyceroldehydes-3-phosphate-dehydrogenase; T_m: melting temperature

(PVDF) membrane. For IGF-1 and VEGF expression analyses, each protein was separated by 16% T tricine-SDS-PAGE and transferred to a 0.22-μm PVDF membrane. The membrane was blocked with 5% (w/v) milk and incubated with primary antibodies for HGF (Santa Cruz, CA), IGF-1 (Santa Cruz), and VEGF (Santa Cruz) overnight at 4 °C. The membrane was then incubated for 1 h with a horseradish peroxidase (HRP)-conjugated secondary antibody at room temperature, washed, developed with the enhanced chemiluminescence Western blotting detection system (Pierce Company Product), and measured by densitometry. Western blotting analysis with a mouse polyclonal antibody against β-actin (Santa Cruz) was used as a protein loading control.

2.10 Nucleus mitotic index in myocardium

Transverse LV cryosections (3 μm) were fixed in acetone (4 °C) for 15 min, and then nonspecific epitope antigens blocked with goat serum at room temperature for 10 min. The sections were incubated with primary antibodies specific to α-sarcomeric actin (Zymed) and Ki-67 (Zeta) at 4 °C overnight, and treated with secondary antibodies conjugated with tetraethyl rhodamine isothiocyanate (TRITC) and FITC, respectively, for 1 h at 37 °C. The nuclei were stained with DAPI (5 μg/ml) for 3 min at room temperature. Fluorescent images were obtained with a Leica TCS SP5 confocal laser scanning microscope and the number of cell nuclei labeled by Ki-67 in myocardium was determined by evaluating approximately 6500 cell nuclei in the border zone and 13000 cell nuclei in the remote myocardium of each section. The numbers were then averaged for hearts treated with or without MSCs. Approximately 13000 cell nuclei in each section were evaluated in sham-operated rat hearts.

2.11 Capillary density

LV cryosections (3 μm) were stained for von Willebrand factor (vWF) using a monoclonal mouse anti-vWF antibody (AbD serotec) as the primary antibody and TRITC-labeled goat anti-mouse antibody as the secondary antibody. Cytoplasmic protein was stained with mouse anti-α-sarcomeric actin antibody (Zymed) followed by FITC-labeled goat anti-mouse antibody. Immunostaining was visualized by Leica DMIRB fluorescence microscopy. The number of capillaries was counted in 20 and 10 random high power fields from the remote myocardium and the border zone in each section, respectively, and the average capillary number per unit area (mm^2) in each group was calculated.

2.12 Statistics

Results are presented as mean±SEM. Survival was analyzed by the standard Kaplan-Meier analysis with log-rank test and χ^2 analysis. Comparison of scar sizes between the two groups was made with the independent-sample T test, and comparisons among the three groups were made with a one-way analysis of variance (ANOVA), followed by the Bonferroni-comparison test. In all tests, differences were considered statistically significant at a value of $P<0.05$.

3 Results

3.1 MSC culture and FACS analysis

The MSCs from 26 animals were successfully cultured and expanded; the average culture duration was (20±3) d. Single cells with a spindle-shaped morphology were observed after 38 h in culture (Fig. 1a in Page 244). They rapidly expanded into colonies

of confluent cells by 5–8 d (Fig. 1b), and the morphology of the passage 1 cells was fairly homogeneous (Fig. 1c). In the lower panel of Fig. 1, the areas under black curves indicated isotype controls, and those under color ones demonstrated MSCs. FACS analysis showed that the majority of passage 2 MSCs expressed CD44 (70.6%) and CD90 (98.0%), but only a small number expressed CD45 (2.2%; a pan-leukocyte marker).

3.2 Scar size and survival

Typical scar areas are shown for the representative samples from CHF and CHF+MSCs groups in Figs. 2a–2c (in Page 244). The sizes of the scars in CHF rats with or without MSC injection were significantly different [(56±0.9) mm^2 vs. (62±1.5) mm^2, $P<0.05$). There were no deaths in the sham-operated rats (0/15); however, 2 CHF rats with MSC injection (10.0%; 2/20) and 7 without MSCs (30.4%; 7/23) died before the end of the experiment. The standard Kaplan-Meier analysis showed that, when compared with CHF rats without MSCs, treatment of CHF rats with MSCs did not significantly increase the percent survival ($P=0.11$).

3.3 Echocardiography

LVEDd changes in systole and in diastole (Fig. 2d) and examples of pulse-wave of Doppler spectra of mitral inflow and aorta outflow (Fig. 2e) are shown for representative animals of the same groups (Fig. 2a). Echocardiographic measurements of LV geometry and function at the 10th week are shown in Table 2. LVEDd markedly increased in CHF rats compared with sham-operated rats ($P<0.01$), and these parameters were significantly attenuated by autologous MSC implantation ($P<0.05$). Rats without MSC treatment had greater cardiac dysfunction compared with sham-operated rats, as evidenced by decreased LVEF and LVFS and by an increased Tei index ($P<0.01$); however, these parameters were significantly improved with autologous MSC implantation ($P<0.05$ vs. CHF group).

3.4 Heart weights and hemodynamics

As shown in Table 2, animals 10 weeks after cardiac injury had a significantly decreased body weight (BW) ($P<0.01$) and elevated heart weight (HW)/BW ratio ($P<0.01$) compared with sham-operated rats. However, the decreased BW and elevated HW/BW ratio were normalized by MSC treatment ($P<0.01$). No significant differences were found in heart rate (HR), mean arterial pressure (MAP), or dP/dt_{max} among the three groups. CHF rats had higher LVEDPs and lower dP/dt_{min} ratios than sham-operated rats ($P<0.01$). However, MSC treatment significantly lowered LVEDP and elevated dP/dt_{min} compared with rats without MSC treatment ($P<0.05$ or $P<0.01$).

Table 2 Changes of parameters for echocardiography, morphology and hemodynamics by autologous MSC implantation

	Sham	CHF	CHF+MSCs
Echocardiography			
n	10	11	10
LVEDd (mm)	6.27±0.15	8.00±0.24[b]	7.18±0.21[ac]
LVEF (%)	87.8±1.7	48.6±3.0[b]	64.4±3.4[bc]
LVFS (%)	52.7±3.1	21.4±2.0[b]	31.0±2.6[bc]
Tei index	0.65±0.03	0.95±0.04[b]	0.81±0.03[ac]
Morphology			
n	10	11	10
BW (g)	515±9	434±11[b]	508±11[d]
HW (mg)	1188±26	1218±33	1249±34
HW/BW	2.34±0.03	2.75±0.07[b]	2.44±0.05[d]
Hemodynamics			
n	10	11	10
HR (beat/min)	387±11	402±12	390±15
MAP (mmHg)	137±3	130±4	138±4
LVEDP (mmHg)	6.1±0.3	15.2±0.6[b]	12.7±0.6[bd]
dP/dt_{max} (mmHg/s)	7843±434	7124±258	7448±208
dP/dt_{min} (mmHg/s)	4039±92	3356±98[b]	3670±85[ac]

LVEDd: LV end-diastolic dimension; LVEF: LV ejection fraction; LVFS: LV fractional shortening; BW: body weight; HW: heart weight; HR: heart rate; MAP: mean arterial pressure; LVEDP: LV end-diastolic pressure; dP/dt_{max}: maximal rate of pressure development; dP/dt_{min}: maximal rate of pressure decline. [a] $P<0.05$ and [b] $P<0.01$ vs. sham; [c] $P<0.05$ and [d] $P<0.01$ vs. CHF. Values are mean±SEM

3.5 Growth factor mRNA expression

Ten weeks after cardiac injury ($n=9$), real-time RT-PCR showed lowered levels in the remote myocardium and elevated levels in the border zone of mRNA expression of IGF-1, HGF, and VEGF-A growth factors (Fig. 3). There were a 0.44-fold decrease in IGF-1, a 0.29-fold decrease in HGF, and a

0.58-fold decrease in VEGF-A in the remote myocardium, and a 1.42-fold in IGF-1, a 1.49-fold in HGF, and a 1.56-fold in VEGF-A in the border zone compared with sham-operated rats (n=7) (P<0.01). However, autologous MSC implantation (n=8) significantly increased mRNA expression of IGF-1, HGF, and VEGF-A by 0.82-fold, 0.37-fold, and 0.88-fold, respectively, in the remote myocardium, and further increased those by 1.81-fold, 1.85-fold, and 2.22-fold, respectively, in the border zone compared with CHF rats without MSCs (P<0.05 or P<0.01).

3.6 Western blotting analysis

Western blotting analyses of IGF-1, HGF, and VEGF-A expression are shown in Fig. 4. Compared with sham-operated animals (n=7) at the 10th week, CHF hearts (n=9) dramatically downregulated the expression of IGF-1, HGF, and VEGF-A (P<0.01) in the remote myocardium, and upregulated the expression of IGF-1, HGF, and VEGF (P<0.01) in the border zone. However, treatment by autologous MSCs (n=8) significantly upregulated the expression of IGF-1, HGF, and VEGF (P<0.05 or P<0.01) in the remote myocardium, and further upregulated the expression of IGF-1, HGF, and VEGF (P<0.05 or P<0.01) in the border zone.

3.7 MSC survival and nuclear mitosis in myocardium

All the cryosections from MSC-implanted hearts were visualized by fluorescence microscopy to detect DAPI staining nuclei. Cells and blood vessels with DAPI staining nuclei can be seen on cryosections (Fig. 5). Nuclear mitosis was clearly detected by Ki-67 labeling. Figs. 6a–6d show an example of a nucleus that is Ki-67 (Fig. 6a, green) positive, DAPI (Fig. 6b, blue), but α-sarcomeric actin (Fig. 6c,

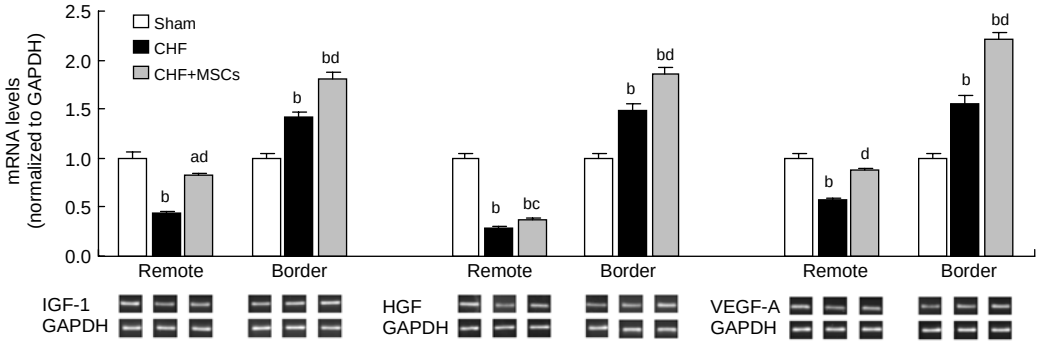

Fig. 3 Effects of MSC implantation on the mRNA expression of growth factors

GAPDH: glyceroldehydes-3-phosphate-dehydrogenase; HGF: hepatocyte growth factor; IGF-1: insulin-like growth factor 1; VEGF-A: vascular endothelial growth factor A. [a] P<0.05 and [b] P<0.01 vs. sham: [c] P<0.05 and [d] P<0.01 vs. CHF. Values are mean±SEM

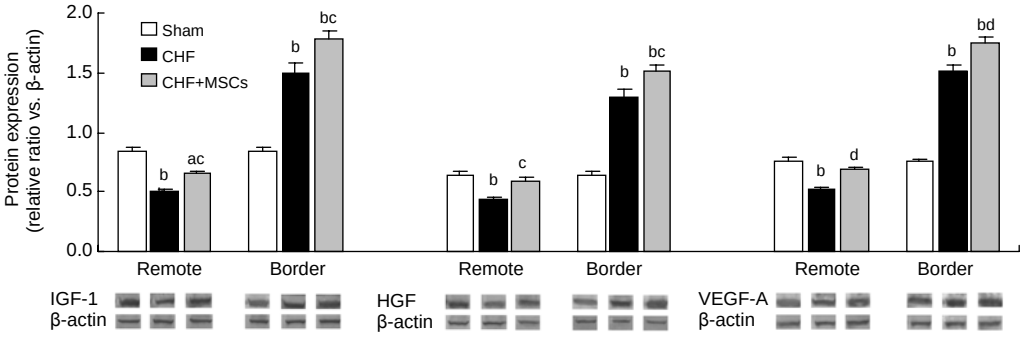

Fig. 4 Effects of MSC implantation on the protein expression of growth factors

HGF: hepatocyte growth factor; IGF-1: insulin-like growth factor 1; VEGF-A: vascular endothelial growth factor A. [a] P<0.05 and [b] P<0.01 vs. sham; [c] P<0.05 and [d] P<0.01 vs. CHF. Values are mean±SEM

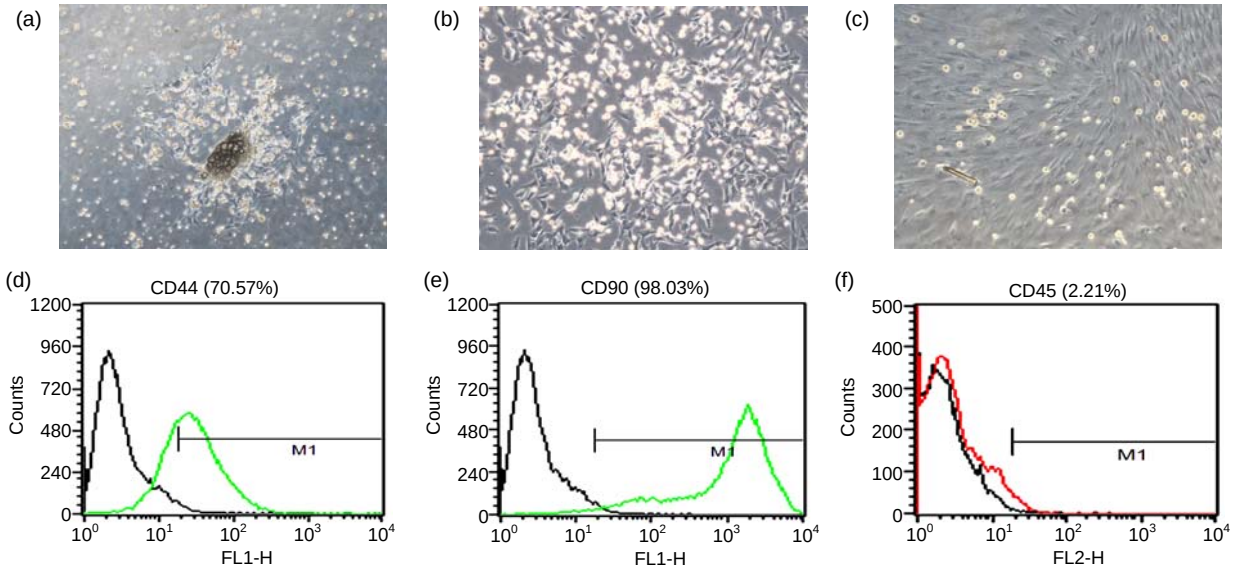

Fig. 1 Characterization of isolated MSCs

Upper panel indicated cells cultured from rat bone marrow after plating at 38 h (a, ×100), 5 d (b, ×100) and 13 d (passage 1) (c, ×100). Lower panel showed FACS analysis with antibodies directed against CD44 (d), CD90 (e), and CD45 (f). The areas under black curves indicated isotype controls, and those under color ones demonstrated MSCs

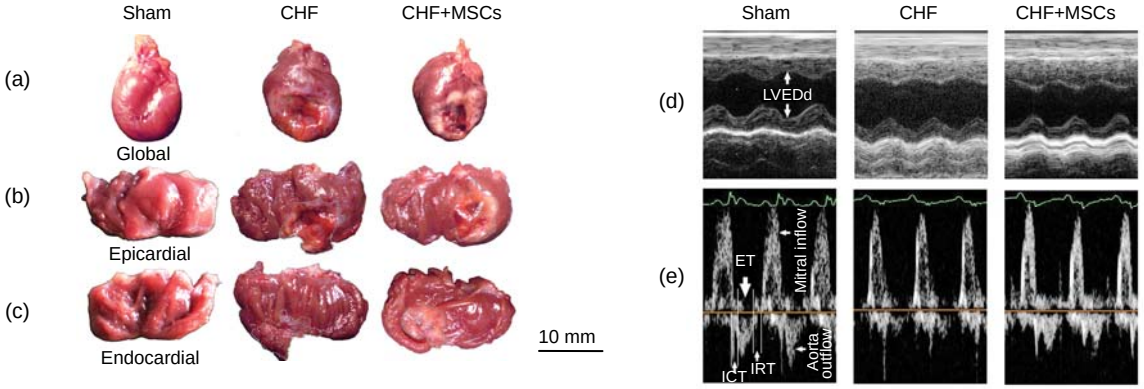

Fig. 2 Scar sizes and echocardiographic images

(a–c) Examples from CHF rats with and without MSCs showed the scar areas on the global (a), epicardial (b) and endocardial (c) aspects of LV. (d) 2D echocardiographic images of LV geometric changes in systole and in diastole and (e) examples of pulse-wave of Doppler spectra of mitral inflow and aorta outflow are shown for representative animals. ET: ejection time; ICT: isovolumic contraction time; IRT: isovolumic relaxation time; LVEDd: LV end diastolic dimension

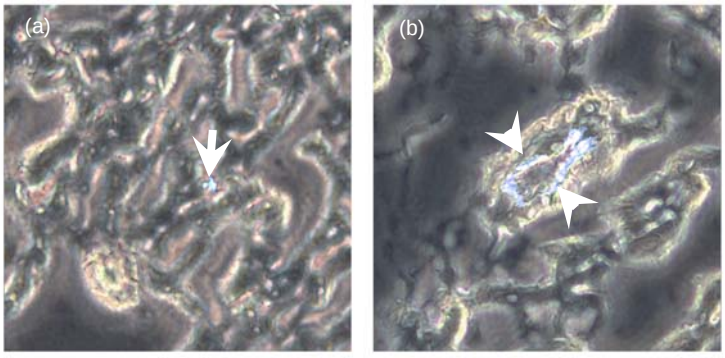

Fig. 5 Detection of implanted MSCs

(a) DAPI-positive nucleus (arrow, ×400) and (b) endothelium with DAPI-positive nuclei in a blood vessel (arrowheads, ×800)

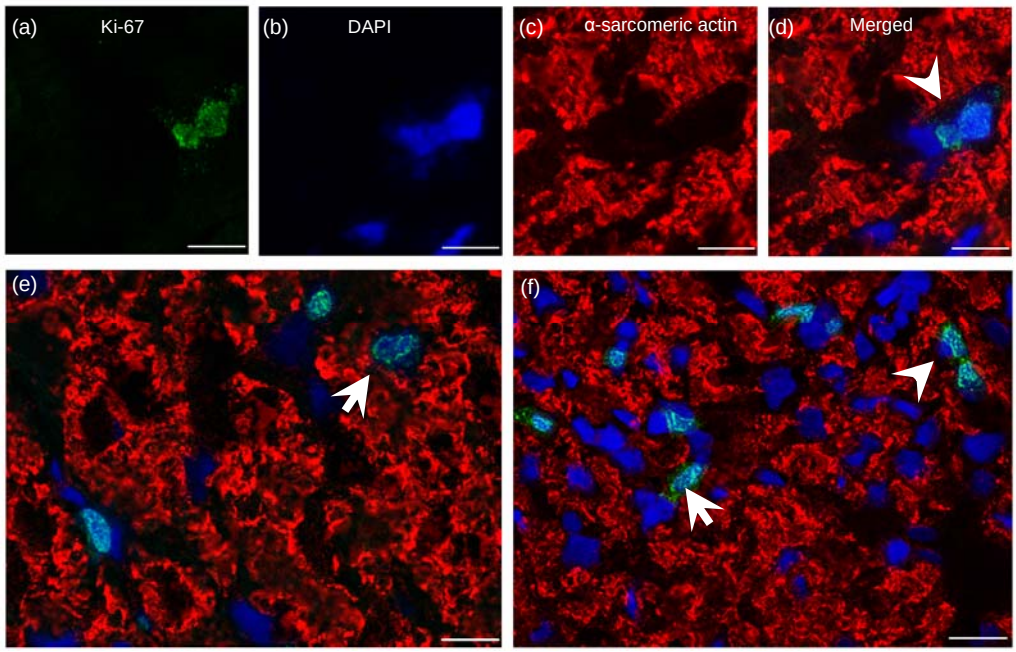

Fig. 6 Ki-67 labeling of mitotic nuclei in myocardium

(a) Ki-67-labeled nucleus (green), (b) DAPI-labeled nuclei (blue), (c) α-sarcomeric actin antibody staining (red) and (d) merged image to illustrate a cycling cell nucleus that is in telophase (the arrowhead indicates the nucleus in caryokinesis). (e) The micrograph demonstrates in the LV myocardium of a sham-operated rat the combined labeling of myocyte cytoplasm by a-sarcomeric actin (red), nuclear staining by DAPI (blue) and cycling nuclei staining with Ki-67 (green; the arrow indicates nucleus in DNA synthesis). (f) The same staining is illustrated in the border zone of an injured heart (the arrowheads show nuclei in caryokinesis). Bars=10 μm

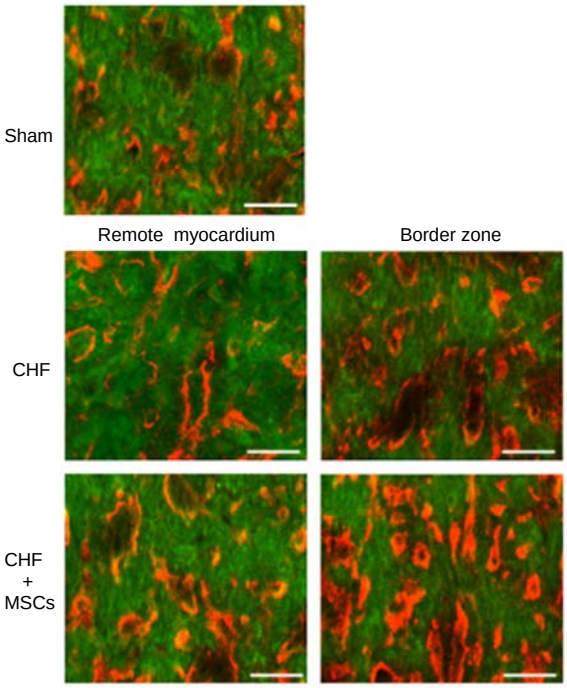

Fig. 7 Micrographs of the example sections from the remote myocardium and the border zone of injured hearts in CHF rats with and without MSCs, stained by a combination of vWF (red) and α-sarcomeric actin (green). Bar=20 μm

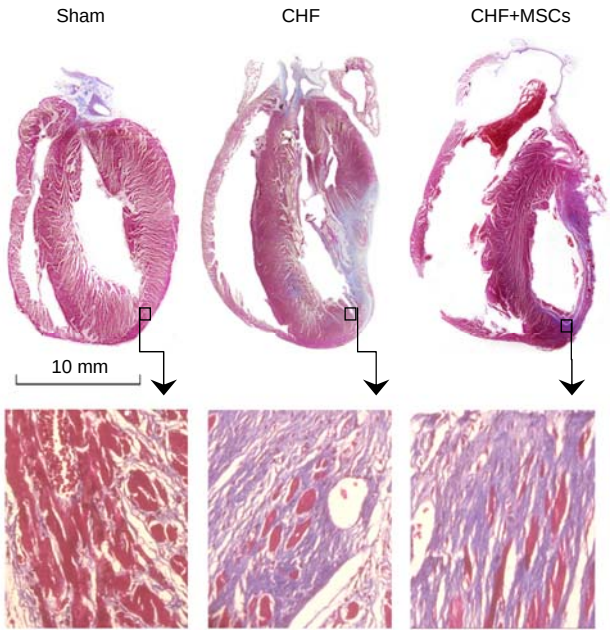

Fig. 8 Upper panel indicates the example mid longitudinal cross-sections from each group; lower panel shows the area of collagen and myocardium in the border zone (stained with Masson's trichrome, ×200)

red) negative, and was in the telophase of the cell cycle (Fig. 6d, merged). The number of cycling cell nuclei in the LV myocardium of sham-operated rats (Fig. 6e) was smaller than that seen in the border zone of damaged hearts (Fig. 6f). Compared with the myocardium of sham-operated hearts (n=7), the border zone in injured hearts (n=7) had a significantly higher nucleus mitotic index per 10000 nuclei (253±18 vs. 88±10, P<0.01). In contrast, the remote myocardium of the injured hearts had a significantly lower mitotic index per 10000 nuclei (49±3 vs. 88±10, P<0.01). Treatment with autologous MSCs (n=7) further increased the nucleus mitotic index in the border zone (324±14 vs. 253±18, P<0.01) and increased that in the remote myocardium (76±5 vs. 49±3, P<0.05).

3.8 Measurement of capillary density

Capillary endothelium was labeled by vWF (Fig. 7) and the number of vessels per unit area (mm^2) counted. Compared with sham-operated rats (n=6), injured hearts (n=6) showed a marked augmentation of neovascularization in the border zone and a marked diminution of neovascularization in the remote myocardium 10 weeks post injury (165±9 vs. 103±6, P<0.01 and 68±5 vs. 103±6, P<0.01, respectively). MSC implantation (n=6) significantly increased the vessel density in the remote myocardium and further increased that in the border zone of CHF rat hearts compared with CHF rats without MSCs (216±6 vs. 165±9, P<0.01 and 94±5 vs. 68±5, P<0.05, respectively).

3.9 Changes of area percentages of collagen and myocardium

Representative areas of collagen and myocardium in border zones in CHF rats with or without MSCs are shown in Fig. 8. Compared with sham-operated animals (n=6), CHF rats (n=6) had a higher area percentage of collagen [(6.8±1.4)% vs. (77.3±4.4)%, P<0.01] and a lower area percentage of myocardium [(92.9±1.7)% vs. (22.5±4.2)%, P<0.05] in the border zone 10 weeks post injury; treatment of CHF rats with autologous MSCs (n=6) significantly decreased area percentage of collagen [(77.3±4.4)% vs. (62.8±3.2)%, P<0.05] and increased area percentage of myocardium [(22.5±4.2)% vs. (36.2±2.9)%, P<0.05].

4 Discussion

Acute myocardial injury is the main cause of CHF, and it is characterized by rapid losses of myocytes and blood vessels. Its progress largely relies on successive self-repair mechanisms in the myocardium. Evidence has shown that the heart is a self-renewing organ and contains a pool of cardiac stem cells, which play a very important role in maintaining heart homeostasis (Kajstura *et al*., 2008). These cardiac stem cells give rise to myocytes, endothelial cells, smooth muscle cells, and fibroblasts during self-repair of myocardium after damage (Anversa *et al*., 2006). Using a rat CHF model induced by cauterization of the heart free wall, the present study demonstrated that autologous MSC implantation promoted expression of IGF-1, HGF, and VEGF growth factors, enhanced cardiomyogenesis and angiogenesis in the failing myocardium, and improved cardiac remodeling and function.

Ten weeks after cardiac injury, cells and blood vessels with DAPI-positive nuclei were seen on the cryosections from MSC-implanted hearts (Fig. 5). However, after they were labeled with Ki-67 and α-sarcomeric actin antibodies together, or vWF antibody alone, and visualized by fluorescence microscopy, the same sections showed dramatically higher levels of cell nucleus mitosis and neovascularization both in the border zone and in the remote myocardium compared with CHF hearts without MSC implantation. Previous studies (Balsam *et al*., 2004; Murry *et al*., 2004) demonstrated that bone marrow stem cells showed little evidence of becoming cardiac muscle cells after they were transplanted into damaged mouse hearts. Implanted MSCs were able to survive in infarcted myocardium for as long as 6 months and express markers that suggest muscle and endothelium phenotypes, but they did not fully evolve into an adult cardiac phenotype (Dai *et al*., 2005). Our present study showed that cauterization-caused CHF significantly increased cell nuclear mitotic index and capillary density in the border zone, and decreased each of them in the remote myocardium when compared with sham-operation. Autologous MSC implantation in CHF dramatically increased cell nucleus mitotic index and capillary density in the remote myocardium, and further increased each of them in the border zone. Nucleus mitosis

indirectly illustrated the capability of myocyte and nonmyocyte proliferation in myocardium (Fig. 6). The newly-generated myocardium definitely included a certain number of myocytes, a proportional quantity of other cells such as fibroblasts, and capillaries, thus enhancing the repair of the damaged myocardium and improving ventricular remodeling and cardiac function. These were evidenced by the changes to HW/BW ratio, scar sizes, hemodynamics and echocardiographic parameters (Table 2), and area percentages of collagen and heart muscle in the border zone (Fig. 8) in rats with CHF.

Cultured MSCs can secrete large amounts of angiogenic, antiapoptotic, and mitogenic factors including IGF-1, HGF, and VEGF (Nagaya *et al*., 2005), and protect the cultured cardiomyocytes from hypoxia/reoxygenation-induced apoptosis through a mitochondria pathway in a paracrine manner (Xiang *et al*., 2009). MSCs can have trophic effects on cells in their vicinity without generating newly differentiated mesenchymal phenotypes, and thus influence the regeneration of cells or tissues by a purely bioactive factor effect (Caplan and Dennis, 2006). IGF-1, a growth hormone mediator, plays an important role in myocardial growth. In the present study, the expression of IGF-1 mRNA and protein was dramatically elevated both in the remote myocardium and in the border zone of CHF rats with MSC addition compared to CHF rats without MSCs. The elevated expression of IGF-1 may benefit the generation of myocardium because cardiac stem cells and early committed cells possess growth factor-receptor systems (Urbanek *et al*., 2005), and the cardioprotective effect of MSCs can be mediated in part by IGF-1, as it exerts marked effects on anti-apoptosis of cardiomyocytes and angiogenesis (Sadat *et al*., 2007), and enhances migration of mature endothelial progenitor cells and tissue resident cardiac stem cells (Urbich *et al*., 2005). HGF can induce cell proliferation and also enhance survival of cardiomyocytes under ischemic conditions (Nakamura *et al*., 2000). In our present study, treatment of CHF rats with autologous MSCs significantly elevated the levels of HGF expression in the failing myocardium. We propose that the HGF secreted by the surviving MSCs or by the triggered cells in their vicinities in both areas of failing myocardium might beneficially have an effect on the amelioration of cardiac remodeling and heart function. VEGF, a highly specific mitogen for vascular endothelial cells, induced endothelial cell proliferation, promoted cell migration, inhibited apoptosis, and played a crucial role in the regulation of vasculogenesis (Pedrotty and Niklason, 2003). In this present study, autologous MSC implantation enhanced VEGF expression in the remote myocardium in CHF rats and further enhanced that in the border zone, so that capillary density significantly increased when compared to CHF rats without MSC treatment. The augmented vascular beds might better supply the cardiac milieu with blood for cardiogenesis and then improve cardiac remodeling and function.

In adult animals, myocardium generation probably results mainly from the division of cardiac stem cells. It is not known whether MSC implantation increased the numbers of cardiac stem cell niches both in the remote myocardium and in the border zone. Future studies will be needed to clarify this question.

References

Amado, L.C., Saliaris, A.P., Schuleri, K.H., St John, M., Xie, J.S., Cattaneo, S., Durand, D.J., Fitton, T., Kuang, J.Q., Stewart, G., *et al*., 2005. Cardiac repair with intramyocardial injection of allogeneic mesenchymal stem cells after myocardial infarction. *Proc. Natl. Acad. Sci. USA*, **102**(32):11474-11479. [doi:10.1073/pnas.0504388102]

Amado, L.C., Schuleri, K.H., Saliaris, A.P., Boyle, A.J., Helm, R., Oskouei, B., Centola, M., Eneboe, V., Young, R., Lima, J.A., *et al*., 2006. Multimodality noninvasive imaging demonstrates in vivo cardiac regeneration after mesenchymal stem cell therapy. *J. Am. Coll. Cardiol.*, **48**(10):2116-2124. [doi:10.1016/j.jacc.2006.06.073]

Anversa, P., Kajstura, J., Leri, A., Bolli, R., 2006. Life and death of cardiac stem cells: a paradigm shift in cardiac biology. *Circulation*, **113**(11):1451-1463. [doi:10.1161/CIRCULATIONAHA.105.595181]

Balsam, L.B., Wagers, A.J., Christensen, J.L., Kofidis, T., Weissman, I.L., Robbins, R.C., 2004. Haematopoietic stem cells adopt mature haematopoietic fates in ischaemic myocardium. *Nature*, **428**(6983):668-673. [doi:10.1038/nature02460]

Caplan, A.I., Dennis, J.E., 2006. Mesenchymal stem cells as trophic mediators. *J. Cell. Biochem.*, **98**(5):1076-1084. [doi:10.1002/jcb.20886]

Chen, S.L., Fang, W.W., Ye, F., Liu, Y.H., Qian, J., Shan, S.J., Zhang, J.J., Chunhua, R.Z., Liao, L.M., Lin, S., *et al*., 2004. Effect on left ventricular function of intracoronary transplantation of autologous bone marrow mesenchymal stem cell in patients with acute myocardial infarction. *Am. J. Cardiol.*, **94**(1):92-95. [doi:10.1016/j.amjcard.2004.03.034]

Dai, W., Hale, S.L., Martin, B.J., Kuang, J.Q., Dow, J.S., Wold,

L.E., Kloner, R.A., 2005. Allogeneic mesenchymal stem cell transplantation in postinfarcted rat myocardium: short- and long-term effects. *Circulation*, **112**(2):214-223. [doi:10.1161/CIRCULATIONAHA.104.527937]

Davani, S., Marandin, A., Mersin, N., Royer, B., Kantelip, B., Herve, P., Etievent, J.P., Kantelip, J.P., 2003. Mesenchymal progenitor cells differentiate into an endothelial phenotype, enhance vascular density, and improve heart function in a rat cellular cardiomyoplasty model. *Circulation*, **108**(Suppl. 1):II253-II258.

Hunt, S.A., 2005. ACC/AHA 2005 guideline update for the diagnosis and management of chronic heart failure in the adult: a report of the American College of Cardiology/American Heart Association Task Force on Practice Guidelines (Writing Committee to Update the 2001 Guidelines for the Evaluation and Management of Heart Failure). *J. Am. Coll. Cardiol.*, **46**(6):e1-82. [doi:10.1016/j.jacc.2005.08.022]

Kajstura, J., Urbanek, K., Rota, M., Bearzi, C., Hosoda, T., Bolli, R., Anversa, P., Leri, A., 2008. Cardiac stem cells and myocardial disease. *J. Mol. Cell. Cardiol*., **45**(4):505-513. [doi:10.1016/j.yjmcc.2008.05.025]

Murry, C.E., Soonpaa, M.H., Reinecke, H., Nakajima, H., Nakajima, H.O., Rubart, M., Pasumarthi, K.B., Virag, J.I., Bartelmez, S.H., Poppa, V., *et al*., 2004. Haematopoietic stem cells do not transdifferentiate into cardiac myocytes in myocardial infarcts. *Nature*, **428**(6983):664-668. [doi:10.1038/nature02446]

Nagaya, N., Kangawa, K., Itoh, T., Iwase, T., Murakami, S., Miyahara, Y., Fujii, T., Uematsu, M., Ohgushi, H., Yamagishi, M., *et al*., 2005. Transplantation of mesenchymal stem cells improves cardiac function in a rat model of dilated cardiomyopathy. *Circulation*, **112**(8):1128-1135. [doi:10.1161/CIRCULATIONAHA.104.500447]

Nakamura, T., Mizuno, S., Matsumoto, K., Sawa, Y., Matsuda, H., 2000. Myocardial protection from ischemia/reperfusion injury by endogenous and exogenous HGF. *J. Clin. Invest.*, **106**(12):1511-1519. [doi:10.1172/JCI10226]

Pedrotty, D.M., Niklason, L.E., 2003. Angiogenesis therapies for cardiovascular disease. *Curr. Opin. Anaesthesiol.*, **16**(1):3-9. [doi:10.1097/00001503-200302000-00002]

Sadat, S., Gehmert, S., Song, Y.H., Yen, Y., Bai, X., Gaiser, S., Klein, H., Alt, E., 2007. The cardioprotective effect of mesenchymal stem cells is mediated by IGF-I and VEGF. *Biochem. Biophys. Res. Commun.*, **363**(3):674-679. [doi:10.1016/j.bbrc.2007.09.058]

Tao, Z.W., Li, L.G., 2007. Cell therapy in congestive heart failure. *J. Zhejiang Univ.-Sci. B*, **8**(9):647-660. [doi:10.1631/jzus.2007.B0647]

Tao, Z.W., Huang, Y.W., Xia, Q., Fu, J., Zhao, Z.H., Lu, X., Bruce, I.C., 2004. Early association of electrocardiogram alteration with infarct size and cardiac function after myocardial infarction. *J. Zhejiang Univ. Sci*., **5**(4):494-498. [doi:10.1631/jzus.2004.0494]

Tao, Z.W., Huang, Y.W., Xia, Q., Xu, Q.W., 2005. Combined effects of ramipril and angiotensin II receptor blocker TCV116 on rat congestive heart failure after myocardial infarction. *Chin. Med. J. (Engl.)*, **118**(2):146-154.

Urbanek, K., Rota, M., Cascapera, S., Bearzi, C., Nascimbene, A., De Angelis, A., Hosoda, T., Chimenti, S., Baker, M., Limana, F., *et al*., 2005. Cardiac stem cells possess growth factor-receptor systems that after activation regenerate the infarcted myocardium, improving ventricular function and long-term survival. *Circ. Res.*, **97**(7):663-673. [doi:10.1161/01.RES.0000183733.53101.11]

Urbich, C., Aicher, A., Heeschen, C., Dernbach, E., Hofmann, W.K., Zeiher, A.M., Dimmeler, S., 2005. Soluble factors released by endothelial progenitor cells promote migration of endothelial cells and cardiac resident progenitor cells. *J. Mol. Cell. Cardiol*., **39**(5):733-742. [doi:10.1016/j.yjmcc.2005.07.003]

Xiang, M.X., He, A.N., Wang, J.A., Gui, C., 2009. Protective paracrine effect of mesenchymal stem cells on cardiomyocytes. *J. Zhejiang Univ-Sci. B*, **10**(8):619-624. [doi:10.1631/jzus.B0920153]